Hindawi
Advances in Civil Engineering
Volume 2022, Article ID 4882095, 10 pages
https://doi.org/10.1155/2022/4882095

Research Article

Effects of Soil Properties and Slope Angle on Deformation and Stability of Cut Slopes

Behailu G. Habtemariam, Kelifa B. Shirago, and Democracy D. Dirate

Institute of Technology, Arba Minch University, Arba Minch, Ethiopia

Correspondence should be addressed to Democracy D. Dirate; democracy.dilla@amu.edu.et

Received 22 February 2022; Revised 28 April 2022; Accepted 9 May 2022; Published 7 June 2022

Academic Editor: Paolo S. Valvo

The impact of soil parameters and slope angle on the deformation and stability of cut slopes is critical for defining road project safety measurement. This study investigates the effect of soil properties and slope angle on the deformation and stability of cut slopes in general and the specific Arba Minch-Chencha upgrading road project. Forty-eight (48) analyses were carried out both in Slope/W and Plaxis 2D software for six cut slopes and analyzed for four different slope angles. Twenty-four (24) dataset samples were collected from six different cut-slope sites. These dataset samples were categorized in two situations, i.e., before and after water saturation for each cut slope. The limit equilibrium method (LEM) comparison clearly showed that the Spencer, Bishop, and Morgenstern-Price methods produced similar FOS. The Ordinary and Janbu approaches, on the other hand, underestimate the FOS. Most LEMs except Ordinary and Janbu methods that estimated higher FOS than finite element method (FEM) analysis. It is observed that the main reasons for the cut-slope instability were the provision of steep cut-slope angles, the existence of a high proportion of fine soil, and moisture content, which was observed in both Plaxis 2D (FEM) and Slope/W (LEM). It was concluded that the slope is more stable for the soil having few fine-grained fractions. Moreover, flattening the slope stabilizes the cut slopes based on the results obtained from both Plaxis 2D and Slope/W.

1. Introduction

The Arba Minch-Chencha road is a national roadway that was built by cutting through the natural terrain of the area and creating a steady slope. Natural disasters such as landslides, soil collapse, and slope failures regularly occur throughout the world. These frequently occur as a result of a lack of forethought while dealing with sloping terrain. The majority of the constructed roads pass through valleys, hilly, and mountainous terrain constructed from cutting and filling of the terrain [1–4].

Evidence indicated that the demand for engineered cut slopes for construction activities grows, and the need for analytical approaches, investigative tools, and stabilization procedures to tackle slope instability requires attention. Man-made slopes usually disrupt the delicate balance of natural soil slopes. Slides can happen in practically every way imaginable, slowly or quickly, and with or without apparent provocation. References [1, 5–7].

Many studies in recent years have been performed to check the stability of the slope using the limit equilibrium method (LEM) or strength reduction methods by finite element method (FEM) [8–13]. An alternative approach was developed by [13–22] to evaluate the slope performance by probabilistic approach. Other researchers like [15, 20, 23–25] evaluated the slope for unsaturated soil.

However, few researchers have addressed the problem of slopes using the strength reduction method by using the finite element method (FEM) to evaluate the slope performance [17, 26–31].

Because the "limit equilibrium technique" and the "finite element method" are still in their early phases of application in many road and infrastructure projects, it is vital to employ these methods to prevent harm after and during construction. However, most of the research deals with either LEM or FEM, to check the stability of the slope, which lacks verification of one method with the other.

The purpose of this study is to investigate and assess the effects of soil properties, water, and slope angles on the stability of cut slopes using the Slope/W (LEM) and Plaxis 2D (FEM) models on the Arba Minch-Chencha route. For each slope, a large number of soil samples were evaluated against input values derived both in the laboratory and in the field. Slope/W and Plaxis 2D software were used to examine the slope geometry with the input parameters. The results can be used to investigate slope performance for various soil types, slope angles, and the impact of water on the cut slopes' slope stability. This research could help assess the performance and validity of slope stability analysis.

2. Materials and Methods

This study was focused on a case-based investigation and analysis of road projects at the Arba Minch-Chencha site. Representative soil samples from six selected sites were collected for laboratory testing to experiment index and engineering properties of the representative soil samples. Limit equilibrium was used to analyze slope stability. [5, 32, 33].

Moreover, Liu et al. [34] analyzed the stability of the slope using limit equilibrium and numerical methods to analyze the slope stability. Many researchers used the strength reduction methods to analyze slopes. [35–38].

2.1. Description of the Study Area. Arba Minch (6° 02′ 24″ to 6° 03′ 57″ N and 37° 33′ 36″ to 37° 35′ 30″ E) and Chencha (6° 14′ 54″ to 6° 15′ 31″ N and 37° 22′ 33″ to 37° 34′ 2″ E) are two towns located in Ethiopia's Southern Nations, Nationalities, and People's (SNNP) regional state (Figure 1). Arba Minch town is located 480 km southwest of Addis Ababa, with Lake Abaya and Lake Chamo to the east. The bottom section of the region is located in the rift valley's plane, while the middle and top portions are located in Ethiopia's southwestern highlands. The Arba Minch-Chencha road section is an extension of the Morka-Gircha-Chencha Road Project, 21 km from Shara Kebele, and the Sodo-Arba Minch main road 15 km from Arba Minch town. The Arba Minch-Chencha upgrading road project begins at a junction on the Arba Minch-Sodo road, which is 470 km from the capital, and connects to the Morka-Gircha-Chencha Road Project, which runs in a westerly direction to the project's end, Wacha Town (Gamo Zone), passing through many rural villages and covering a total length of 108.6 km.

2.2. Sampling, Sample Collection, and Laboratory Tests. The soil samples for this investigation were obtained from the Chano-Chencha section of the existing gravel road from Arba Minch to Chencha. Six sampling areas were selected from various points along the road to reflect all soils found in the surrounding based on a preliminary site study. A total of twenty-four pits were excavated to a maximum depth of three meters to visually observe the subsurface condition and collect representative samples (Figure 2). For this study, good-quality disturbed soil samples were easily collected,

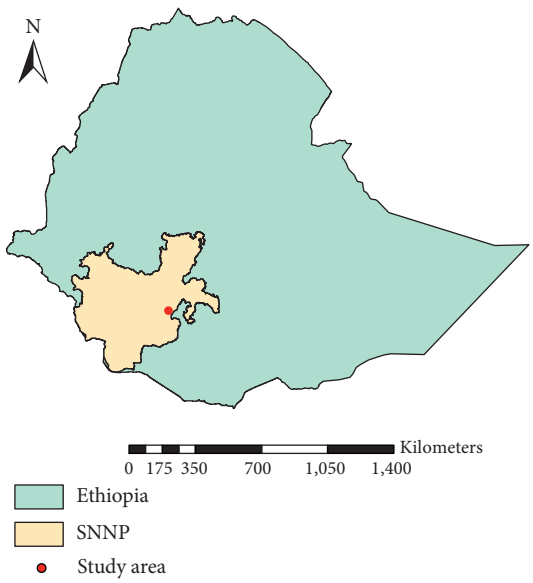

Figure 1: Location of the study area.

transported carefully to a laboratory for testing, and then tested to determine engineering properties, moisture content, specific gravity, Atterberg limit, grain size analysis, direct shear, and one-dimensional consolidation [39].

The specific gravity of the study area ranges from 2.67 to 2.73. The soils for almost all samples were fine-grained. From the sieve size analysis results, clay content ranges from 1.52% to 12.14%, silt content ranges from 30.64% to 59.86%, sand fractions range from 28.80% to 58.45%, and gravel content ranges from 1.5% to 9.2%. The soil in slope-1 was classified as silty or clayey gravel and sand in the crust slope using the American Association of State Highway and Transportation Officials (AASHTO) classification system. The soil slope-2 is classified as low-plastic silt and high-plastic silt, with low-plastic silt at the mid-slope and high-plastic silt at the toe slope. Slope-3 and slope-6 were grouped under silty or clayey gravel and sand at the crust slope and low-plastic silt at mid-slope and toe slope. The soil profile of slope-4 was also classified as high-plastic silt, and slope-5 was classified as having low-plastic silt and high-plastic silt. The input data for the analysis of LEM and FEM were determined from in situ and laboratory tests. The shear strength parameters were determined from a remolded sample. Young's modulus and Poisson's ratio were determined from an unconsolidated undrained test of the triaxial test. Young's modulus is varied with water content, so to be conservative, Young's modulus for the saturated condition is taken for both the analysis of before and after saturation condition. Table 1 shows laboratory and field test results for the input parameters for analysis of the model.

2.3. Analysis Methods. Methods of limit equilibrium using Slope/W are as follows: the factor of safety is calculated from a two-dimensional equilibrium condition such that the factor of safety is the ratio of resistance force or moment to driving force or moment.

Figure 2: Test pit for a sampling of the soil.

Table 1: Input parameters for LEM and FEM.

Parameters	Slope-1	Slope-2	Slope-3	Slope-4	Slope-5	Slope-6
Bulk unit weight, γ(kN/m^3)	18.05	18.27	18.29	18.75	18.22	18.10
Saturated unit weight, γ_{sat} (kN/m3)	18.62	18.32	18.51	18.36	18.43	18.21
Young's modulus, E	19,834	21,678	22,794	20,130	23,485	21,233
Poison's ratio, υ	0.35	0.35	0.30	0.35	0.35	0.30
Cohesion before saturation, (kN/m^2)	9.30	11.52	14.50	14.15	14.74	14.80
Cohesion after saturation, (kN/m^2)	7.26	10.19	11.28	10.19	12.33	10.16
Friction angle before saturation, (°)	23.8	21.1	21.7	19.0	24.4	22.9
Friction angle after saturation, (°)	19.1	14.9	16.8	16.3	19.2	17.7

$$\text{FOS} = \frac{\text{resisting force (moment)}}{\text{driving force (moment)}}. \quad (1)$$

The Slope/W program was used to build the geometry. Morgenstern-Price, Ordinary, Spencer, Bishop, and Janbu methods were used to solve FOS. The slope stability was further assessed using Plaxis 2D, which is a finite element method, and the factor of safety was determined by the strength reduction technique.

For both LEM and FEM, the input parameters were carefully determined from laboratory testing.

2.4. Strength Parameters (C, ϕ). The shear strength parameters were determined from representative testing of the soil in the laboratory. The samples were prepared by remolding the soil samples using their natural moisture content and in situ unit weight. Three tests were conducted with parrying vertical stress such that the second sample is equivalent to the in situ vertical stress of the soil sample and applying shear stress until the sample failed.

The shear strength was determined for natural moisture content and saturated condition, and for the saturated condition, the soil sample was soaked till the sample is saturated. For a saturated soil sample, an additional increase in the stress on the sample is proportional to an increase in pore water pressure, and in other words, $B = 1$ [40].

$$\Delta U = B\sigma_3. \quad (2)$$

2.5. Unit Weight (γ). The unit weight of the soil was determined using a core cutter sampler, by dividing the weight of a known volume of the sample by the volume of the soil.

Young's modulus and Poisson's ratio (E, υ).

Young's modulus and Poisson's ratio were determined by conducting unconsolidated undrained triaxial tests on undisturbed soil samples using a Shelby sampler. The vertical load was applied until the samples failed, so the modulus of elasticity and Poisson's ratio of the sample at a different location are determined using equations (3) and (4).

$$E = \frac{\text{stress at failure } (\sigma)}{\text{strain } (\epsilon_z)}, \quad (3)$$

$$U = \frac{\text{Lateral strain } (\epsilon_r)}{\text{Normal strain } (\epsilon_z)}. \quad (4)$$

3. Results and Discussion

In this study, the critical slope and stability of the slope were analyzed for different soils, which were achieved through the accurate determination of input parameters.

Before the laboratory test of soil samples, a field assessment was performed to recognize prone soil slopes. Subsequently, there will be in situ tests to determine the density of the field and collect representative samples for laboratory testing. We determine the input parameters such as cohesion, friction angle, Atterberg limit, and Young's modulus for analysis of the model slope. The numerical simulation approaches of the finite element method (FEM) and limit equilibrium method (LEM) were employed to investigate slopes with specified geometry [41].

3.1. Numerical Results. The stability of the slopes was analyzed using the FEM and LEM for comparison and verification of the slope condition. Using the LEM and FEM software, factor of safety (FOS) and slope deformation were determined. The comparison was made using modeling data from Plaxis 2D (FEM-based) and Geo-Slope 2012 (LEM-based) software. Furthermore, the condition of the slope before saturation and after saturation was analyzed so that the stability of the slope and the deformation of the corresponding state of the soil were determined. The input parameters for both LEM and FEM analysis were carefully determined from both laboratory and field tests. The whole set of the input parameters for both Plaxis 2D and Slope/W software for specified slopes was used to model the geometry of the slope.

3.2. Plaxis 2D Analysis. Plaxis 2D is a very useful finite element software to solve the FOS of the slope using the strength reduction method at the finite element level, whereas LEM analyzes the stability of the slope from equilibrium condition for the resisting force or moment to force or moment causing instability. From the analysis of the Plaxis 2D, it is indicated that as the water level rises, the slope deforms more; this indicated that the slope becomes more unstable with high water content. Many researchers like [42] indicated that water hurts the long-term stability of the embankment due to the development of pore water pressure. As depicted in Figure 3, the most extreme total displacement for the slope angle (1H: 1V) is 905×10^{-3} m as determined by the shear strength parameters after saturation.

3.2.1. Characteristic Slope-1. The FOS and deformation of CS1 for different slope angles before saturation and after saturation are shown in Table 2. After modification of the slope, it showed much deformation, which indicated the soil is more deformable both before and after saturation conditions.

3.2.2. Characteristic Slope-2. For slope angles of (1H: 1V), (1.5H: 1V), (2H: 1V), and (2.5H: 1V), Table 3 shows FOS and slope deformation values for slope-2 using shear parameters by Plaxis 2D for the case of before saturation and after saturation.

3.2.3. Characteristic Slope-3. Table 4 shows the FOS and slope deformation values for slope-3 using shear parameters by Plaxis 2D for the case of before saturation and after saturation.

3.2.4. Characteristic Slope-4. The FOS before saturation for slope (1H: 1V), (1.5H: 1V), (2H: 1V), and (2.5H: 1V) was 1.205, 1.345, 1.490, and 1.674, respectively, while the FOS of the fully saturated condition was 0.977, 1.154, 1.385, and 1.480, respectively. The highest extreme total displacement determined using shear parameters after saturation for a slope angle of (1H: 1V) is $943 \times \times 10^{-3}$ m. Table 5 shows FOS and slope deformation values for slope-4 using shear parameters by Plaxis 2D for the case of before saturation and after saturation.

3.2.5. Characteristic Slope-5. Table 6 shows FOS and slope deformation values for slope-5 using shear parameters by Plaxis 2D for the case of before saturation and after saturation.

The maximum total deformation attained using shear parameters (1H: 1V), (1.5H: 1V), (2H: 1V), and (2.5H: 1V) is larger after saturation. In contrast, the maximum total deformation attained using shear parameters before saturation is more negligible, and the factor of safety value is the opposite. Using the shear characteristics after saturation, the maximum extreme total displacement for the slope angle (1H: 1V) is 996×10^{-3} m.

3.2.6. Characteristic Slope-6. Table 7 shows FOS and slope deformation values for slope-6 using shear parameters by Plaxis 2D for the case of before saturation and after saturation.

The maximum total deformation attained using shear parameters for slope is reduced when the slope angle flattens, which is analogous to many researchers. Moreover, both horizontal deformation and vertical deformation increased after saturation. In contrast, the maximum total deformation attained using shear parameters before saturation is more negligible, the factor of safety value is the opposite, and this suggested that deformation and factor of safety are inversely proportional for the slope under dry conditions and saturated conditions (Table 7). Using the shear characteristics after saturation, the maximum total displacement for the slope angle (1H: 1V) is 958×10^{-3} m.

3.3. Slope/W Analysis. Slope/W analyzes the stability of the slope using the LEM. Five different methods (Sarma, Bishop, Ordinary, Janbu, and Morgenstern-Price) were taken to check the stability of the slopes. Each method analyzes the slopes based on equilibrium conditions, some methods considered equilibrium for the moment and force in the horizontal and vertical direction (Sarma and Morgenstern-Price), others considered only moment equilibrium (Ordinary and Bishop), and Janbu considered force equilibrium in the horizontal and vertical directions [2].

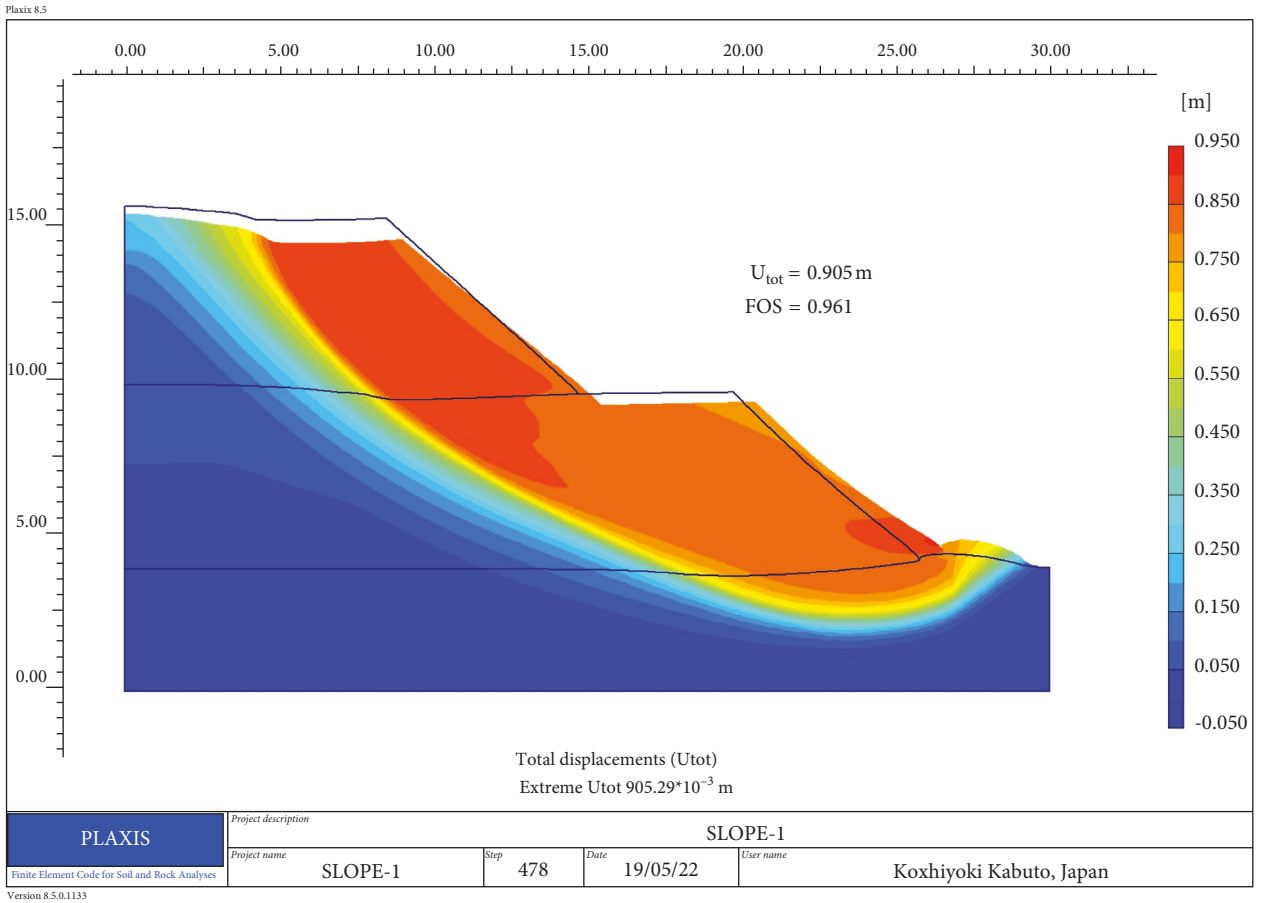

Figure 3: Displacement of CS1 for a slope angle of (1H : 1V).

Table 2: FOS and slope deformation values for slope-1 by Plaxis 2D before and after saturation.

Slope angle	Before saturation				After saturation			
	Horizontal deformation U_x (m)	Vertical deformation U_y (m)	Total deformation U_{tot} (m)	Factor of safety (FOS)	Horizontal deformation U_x (m)	Vertical deformation U_y (m)	Total deformation U_{tot} (m)	Factor of safety (FOS)
1H: 1V	0.553	0.441	0.577	1.039	0.894	0.737	0.905	0.961
1.5H: 1V	0.441	0.376	0.459	1.302	0.621	0.544	0.662	1.152
2H: 1V	0.326	0.310	0.376	1.621	0.483	0.429	0.534	1.342
2.5H: 1V	0.288	0.289	0.346	1.743	0.390	0.359	0.443	1.534

Table 3: FOS and slope deformation values for slope-2 by Plaxis 2D before and after saturation.

Slope angle	Before saturation				After saturation			
	Horizontal deformation U_x (m)	Vertical deformation U_y (m)	Total deformation U_{tot} (m)	Factor of safety (FOS)	Horizontal deformation U_x (m)	Vertical deformation U_y (m)	Total deformation U_{tot} (m)	Factor of safety (FOS)
1H: 1V	0.477	0.406	0.504	1.128	0.902	0.756	0.933	0.956
1.5H: 1V	0.402	0.368	0.441	1.309	0.808	0.667	0.844	1.055
2H: 1V	0.338	0.332	0.402	1.550	0.542	0.500	0.614	1.163
2.5H: 1V	0.274	0.289	0.344	1.657	0.410	0.395	0.483	1.304

Table 4: FOS and slope deformation values for slope-3 by Plaxis 2D before and after saturation.

Slope angle	Before saturation				After saturation			
	Horizontal deformation U_x (m)	Vertical deformation U_y (m)	Total deformation U_{tot} (m)	Factor of safety (FOS)	Horizontal deformation U_x (m)	Vertical deformation U_y (m)	Total deformation U_{tot} (m)	Factor of safety (FOS)
1H: 1V	0.538	0.422	0.538	1.207	0.908	0.789	0.931	0.937
1.5H: 1V	0.360	0.376	0.435	1.364	0.774	0.699	0.847	1.138
2H: 1V	0.302	0.345	0.384	1.525	0.613	0.571	0.692	1.433
2.5H: 1V	0.175	0.226	0.271	1.741	0.407	0.403	0.491	1.515

Table 5: FOS and slope deformation values for slope-4 by Plaxis 2D before and after saturation.

Slope angle	Before saturation				After saturation			
	Horizontal deformation U_x (m)	Vertical deformation U_y (m)	Total deformation U_{tot} (m)	Factor of safety (FOS)	Horizontal deformation U_x (m)	Vertical deformation U_y (m)	Total deformation U_{tot} (m)	Factor of safety (FOS)
1H: 1V	0.599	0.466	0.632	1.205	0.917	0.769	0.943	0.977
1.5H: 1V	0.351	0.354	0.416	1.345	0.592	0.562	0.662	1.154
2H: 1V	0.234	0.267	0.302	1.490	0.438	0.396	0.487	1.385
2.5H: 1V	0.200	0.238	0.268	1.674	0.268	0.287	0.339	1.480

Table 6: FOS and slope deformation values for slope-5 by Plaxis 2D before and after saturation.

Slope angle	Before saturation				After saturation			
	Horizontal deformation U_x (m)	Vertical deformation U_y (m)	Total deformation U_{tot} (m)	Factor of safety (FOS)	Horizontal deformation U_x (m)	Vertical deformation U_y (m)	Total deformation U_{tot} (m)	Factor of safety (FOS)
1H: 1V	0.463	0.464	0.518	1.205	0.958	0.847	0.996	0.968
1.5H: 1V	0.333	0.358	0.407	1.396	0.629	0.607	0.715	1.197
2H: 1V	0.234	0.271	0.309	1.613	0.409	0.432	0.506	1.316
2.5H: 1V	0.228	0.286	0.321	1.806	0.273	0.323	0.368	1.460

Table 7: FOS and slope deformation values for slope-6 by Plaxis 2D before and after saturation.

Slope angle	Before saturation				After saturation			
	Horizontal deformation U_x (m)	Vertical deformation U_y (m)	Total deformation U_{tot} (m)	Factor of safety (FOS)	Horizontal deformation U_x (m)	Vertical deformation U_y (m)	Total deformation U_{tot} (m)	Factor of safety (FOS)
1H: 1V	0.732	0.562	0.734	1.268	0.939	0.797	0.958	0.940
1.5H: 1V	0.602	0.514	0.668	1.562	0.781	0.742	0.870	1.192
2H: 1V	0.314	0.464	0.464	1.694	0.639	0.587	0.709	1.409
2.5H: 1V	0.231	0.290	0.322	1.859	0.383	0.378	0.458	1.495

From the results of the Slope/W, slip surfaces for slopes CS1(a), CS2(b), CS3(c), CS4(d), CS5(e), and CS6(f) for the case of slope angle (1H: 1V) after saturation of the soil are shown in Figure 4.

The FOS for slopes CS1(a), CS2(b), CS3(c), CS4(d), CS5(e), and CS6(f) for different slope angles before and after saturation is indicated in Tables 8–13, respectively, using the different LEM methods.

The results presented in Tables 8–13 clearly show that the FOS is higher than 1 for the case of before saturation for the given different slope angles. This indicates that all slopes are considered stable under dry conditions. However, FOS values for all six slopes for the geometric slope angle of (1H: 1V) with water saturation are less than 1, and this depicts that the slopes are not stable under saturated conditions.

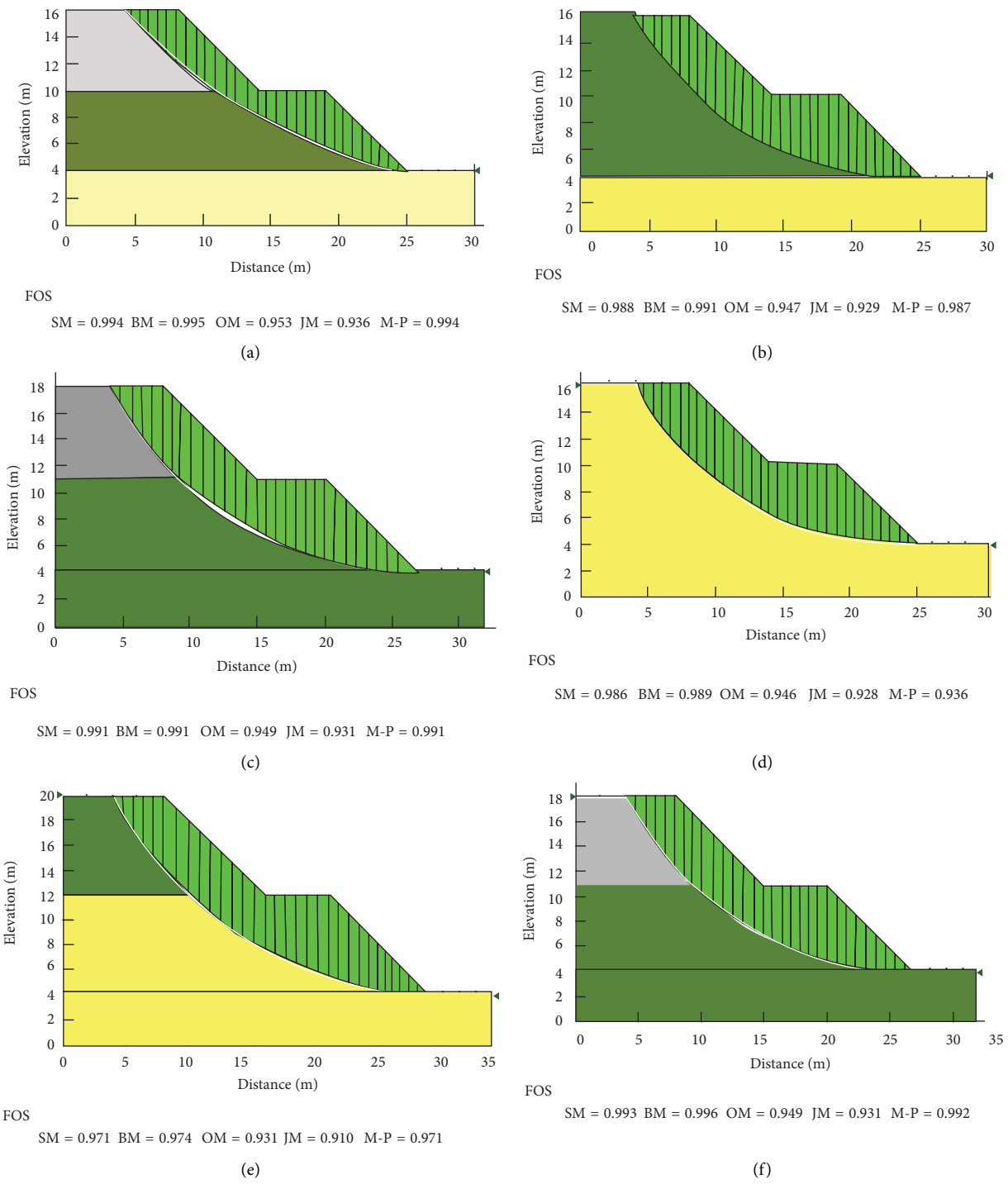

Figure 4: Slip surface of the slopes after saturation for the slope angle (1H: 1V): (a) CS1; (b) CS2; (c) CS3; (d) CS4; (e) CS5; (f) CS6.

Table 8: FOS values for slope-1 for different slope angles before and after saturation.

Slope angle	Before saturation FOS					After saturation FOS				
	Bishop	Spencer	Ordinary	Janbu	M-P	Bishop	Spencer	Ordinary	Janbu	M-P
1H: 1V	1.129	1.129	1.074	1.056	1.129	0.995	0.994	0.953	0.936	0.994
1.5H: 1V	1.375	1.375	1.345	1.325	1.375	1.253	1.252	1.122	1.194	1.252
2H: 1V	1.769	1.767	1.71	1.676	1.767	1.406	1.405	1.347	1.321	1.405
2.5H: 1V	1.894	1.892	1.757	1.728	1.892	1.642	1.641	1.559	1.528	1.641

Table 9: FOS values for slope-2 for different slope angles before and after saturation.

Slope angle	Before saturation FOS					After saturation FOS				
	Bishop	Spencer	Ordinary	Janbu	M-P	Bishop	Spencer	Ordinary	Janbu	M-P
1H: 1V	1.175	1.171	1.115	1.095	1.171	0.991	0.988	0.947	0.929	0.987
1.5H: 1V	1.421	1.42	1.362	1.331	1.42	1.118	1.115	1.053	1.028	1.115
2H: 1V	1.7	1.699	1.61	1.572	1.699	1.221	1.221	1.177	1.141	1.221
2.5H: 1V	1.807	1.807	1.741	1.702	1.807	1.391	1.393	1.339	1.297	1.393

Table 10: FOS values for slope-3 for different slope angles before and after saturation.

Slope angle	Before saturation FOS					After saturation FOS				
	Bishop	Spencer	Ordinary	Janbu	M-P	Bishop	Spencer	Ordinary	Janbu	M-P
1H: 1V	1.268	1.263	1.209	1.186	1.263	0.991	0.988	0.947	0.929	0.987
1.5H: 1V	1.442	1.438	1.358	1.328	1.438	1.118	1.115	1.053	1.028	1.115
2H: 1V	1.657	1.653	1.547	1.511	1.653	1.221	1.221	1.177	1.141	1.221
2.5H: 1V	1.916	1.915	1.786	1.745	1.915	1.391	1.393	1.339	1.297	1.393

Table 11: FOS values for slope-4 for different slope angles before and after saturation.

Slope angle	Before saturation FOS					After saturation FOS				
	Bishop	Spencer	Ordinary	Janbu	M-P	Bishop	Spencer	Ordinary	Janbu	M-P
1H: 1V	1.259	1.255	1.205	1.18	1.254	0.989	0.986	0.946	0.928	0.998
1.5H: 1V	1.468	1.464	1.391	1.357	1.464	1.217	1.213	1.148	1.122	1.213
2H: 1V	1.636	1.633	1.533	1.495	1.633	1.489	1.487	1.395	1.361	1.487
2.5H: 1V	1.829	1.826	1.701	1.659	1.826	1.59	1.587	1.473	1.439	1.588

Table 12: FOS values for slope-5 for different slope angles before and after saturation.

Slope angle	Before saturation FOS					After saturation FOS				
	Bishop	Spencer	Ordinary	Janbu	M-P	Bishop	Spencer	Ordinary	Janbu	M-P
1H: 1V	1.231	1.23	1.17	1.139	1.229	0.974	0.971	0.931	0.91	0.971
1.5H: 1V	1.525	1.527	1.448	1.409	1.527	1.207	1.205	1.139	1.114	1.204
2H: 1V	1.771	1.772	1.683	1.64	1.772	1.407	1.406	1.314	1.283	1.405
2.5H: 1V	1.983	1.985	1.899	1.85	1.984	1.601	1.601	1.502	1.467	1.601

Table 13: FOS values for slope-6 for different slope angles before and after saturation.

Slope angle	Before saturation FOS					After saturation FOS				
	Bishop	Spencer	Ordinary	Janbu	M-P	Bishop	Spencer	Ordinary	Janbu	M-P
1H: 1V	1.307	1.303	1.245	1.215	1.303	0.996	0.993	0.949	0.931	0.992
1.5H: 1V	1.613	1.609	1.518	1.481	1.609	1.253	1.25	1.18	1.153	1.25
2H: 1V	1.834	1.834	1.715	1.672	1.834	1.444	1.441	1.346	1.316	1.441
2.5H: 1V	2.014	2.013	1.889	1.846	2.013	1.614	1.614	1.513	1.481	1.614

4. Conclusions and Recommendations

4.1. Conclusions. From the modeling results, the causes of cut-slope instability, the cut-slope geometry, water content, and soil properties were investigated.

The minimal factor of safety value in the result table clearly illustrates that the factor of safety reduces as the amount of water in the slope increases, which indicated that the slope becomes more unstable as the number of water increases. As the slope angle decreases, the amount of factor of safety increases.

The steepness was the primary cause of instability and then are a lower factor of safety and a higher maximum predicted displacement of a cut slope. Moreover, flattening the slope from (1H: 1V) to (1.5H: 1V), (2H: 1V), and (2.5H: 1V) stabilizes the slopes in both Plaxis 2D and Slope/W.

When the modeling results were compared, it was demonstrated that the Spencer, Bishop, and Morgenstern-

Price approaches produced nearly the same FOS. However, Janbu and Ordinary methods may underestimate the FOS ranging from 5% to 6%. The LEM estimates higher FOS than FEM analysis, except for the Janbu and Ordinary methods. The Janbu and Ordinary methods, when compared to the FEM, underestimate FOS by up to 7% on average.

5. Recommendations

The factors of safety and cut-slope displacements were calculated using finite element analysis methods and the two-dimensional limit equilibrium method. To provide a more realistic simulation of the problem, the slope side effect should be incorporated into three-dimensional finite element analysis methods.

In this study, two conditions of the soil state condition are considered: a dry condition and a saturated condition, which are extreme conditions, so it is recommended to check the unsaturated stability condition considering the suction stress in unsaturated soil, the soil-water characteristic curve (SWCC), and the suction stress characteristic curve (SSCC) of the unsaturated soil obtained from the study area. [24, 43–45].

Data Availability

The data used to support the findings of this study are available from the corresponding author upon request.

Conflicts of Interest

The authors declare that they have no conflicts of interest.

Acknowledgments

The authors would like to extend their heartfelt gratitude to the Arba Minch University staff for their support at our disposal for laboratory testing and manuscript preparation for the accomplishment of this paper. This work was a duty as an academic job in our institute, Arba Minch University.

References

[1] J. B. Ritter, *Landslides and Slope Stability Analysis*, Landslides, 2004.

[2] L. W. Abramson, T. S. Lee, S. Sharma, and G. M. Boyce, *Slope Stability and Stabilization Methods*, John Wiley & Sons, New York, 2002.

[3] R. N. Chowdhury, "Propagation of failure surfaces in natural slopes," *Journal of Geophysical Research: Solid Earth*, vol. 83, no. B12, pp. 5983–5988, 1978.

[4] E. Bromhead, "The stability of slopes," *The Stability of Slopes*, Taylor & Francis, Milton Par, 1992.

[5] A. W. Bishop, "The influence of progressive failure on the choice of the method of stability analysis," *Géotechnique*, vol. 21, no. 2, pp. 168–172, 1971.

[6] A. W. Bishop and N. Morgenstern, "Stability coefficients for earth slopes," *Géotechnique*, vol. 10, no. 4, pp. 129–153, 1960.

[7] D. Sterpi and V. P. Singh, "Analysis of gradual earth-dam failure," *Water (Switzerland)*, vol. 12, no. 1, pp. 1–15, 2020.

[8] K. M. Bushira, Y. B. Gebregiorgis, R. K. Verma, and Z. Sheng, "Cut soil slope stability analysis along national Highway at wozeka-gidole road, Ethiopia," *Modeling Earth Systems and Environment*, vol. 4, no. 2, pp. 591–600, 2018.

[9] M. Mortazavi Zanjani, A. Soroush, and M. Khoshini, "Two-dimensional numerical modeling of fault rupture propagation through earth dams under steady state seepage," *Soil Dynamics and Earthquake Engineering*, vol. 88, pp. 60–71, 2016.

[10] Jn. Albataineh, *Slope Stability Analysis using 2D And 3D Method*, pp. 1–220, Buchtel Ave, Akron, 2006.

[11] K. S. Kahatadeniya, P. Nanakorn, and K. M. Neaupane, "Determination of the critical failure surface for slope stability analysis using ant colony optimization," *Engineering Geology*, vol. 108, no. 1-2, pp. 133–141, 2009.

[12] D. G. Fredlund and J. Krahn, "Comparison of slope stability methods of analysis," *Canadian Geotechnical Journal*, vol. 14, no. 3, pp. 429–439, 1977.

[13] C. Reale, J. Xue, Z. Pan, and K. Gavin, "Deterministic and probabilistic multi-modal analysis of slope stability," *Computers and Geotechnics*, vol. 66, pp. 172–179, 2015.

[14] J. T. Christian, C. C. Ladd, and G. B. Baecher, "Reliability applied to slope stability analysis," *Journal of Geotechnical Engineering*, vol. 120, no. 12, pp. 2180–2207, 1994.

[15] A. Gholampour and A. Johari, "Reliability-based analysis of braced excavation in unsaturated soils considering conditional spatial variability," *Computers and Geotechnics*, vol. 115, Article ID 103163, 2019.

[16] C. Reale, K. Gavin, L. J. Prendergast, and J. Xue, "Multi-modal reliability analysis of slope stability," *Transportation Research Procedia*, vol. 14, pp. 2468–2476, 2016.

[17] K. Nitzsche, I. Herle, K. Nitzsche, and I. Herle, "Strain-dependent slope stability," *Acta Geotechnica*, vol. 15, no. 11, pp. 3111–3119, 2020.

[18] D. V. Griffiths and G. A. Fenton, "Probabilistic slope stability analysis by finite elements," *Journal of Geotechnical and Geoenvironmental Engineering*, vol. 130, no. 5, pp. 507–518, 2004.

[19] S. S. Kar and L. B. Roy, "Probabilistic based reliability slope stability analysis using FOSM, FORM, and MCS," *Engineering, Technology & Applied Science Research*, vol. 12, no. 2, pp. 8236–8240, 2022.

[20] S. Oh and N. Lu, "Slope stability analysis under unsaturated conditions: case studies of rainfall-induced failure of cut slopes," *Engineering Geology*, vol. 184, pp. 96–103, 2015.

[21] H. Rafiei Renani, C. D. Martin, P. Varona, and L. Lorig, "Stability analysis of slopes with spatially variable strength properties," *Rock Mechanics and Rock Engineering*, vol. 52, no. 10, pp. 3791–3808, 2019.

[22] E. H. Vanmarcke, "Reliability OF earth slopes," *Journal of the Geotechnical Engineering Division*, vol. 103, no. 11, pp. 1247–1265, 1977.

[23] A. Gholampour and A. Johari, "Reliability analysis of a vertical cut in unsaturated soil using sequential Gaussian simulation," *Scientia Iranica*, vol. 26, no. 3, pp. 1214–1231, 2019.

[24] L. Batali and C. Andreea, "Slope stability analysis using the unsaturated stress analysis. Case study," *Procedia Engineering*, vol. 143, no. 3, pp. 284–291, 2016.

[25] S. E. Cho and S. R. Lee, "Instability of unsaturated soil slopes due to infiltration," *Computers and Geotechnics*, vol. 28, no. 3, pp. 185–208, 2001.

[26] X. Guo and D. Dias, "Kriging based reliability and sensitivity analysis - application to the stability of an earth dam,"

Computers and Geotechnics, vol. 120, no. Apr, Article ID 103411, 2020.

[27] R. Afiri and S. Gabi, "Finite element slope stability analysis of Souk Tleta dam by shear strength reduction technique," *Innovative Infrastructure Solutions*, vol. 3, no. 1, pp. 6–70, 2018.

[28] F. Tschuchnigg, H. F. Schweiger, and S. W. Sloan, "Slope stability analysis by means of finite element limit analysis and finite element strength reduction techniques. Part I: numerical studies considering non-associated plasticity," *Computers and Geotechnics*, vol. 70, pp. 169–177, 2015.

[29] G. p. Tang, L. h. Zhao, L. Li, and F. Yang, "Stability charts of slopes under typical conditions developed by upper bound limit analysis," *Computers and Geotechnics*, vol. 65, pp. 233–240, 2015.

[30] M. A. Idris, D. Saiang, and E. Nordlund, "Probabilistic analysis of open stope stability using numerical modelling," *International Journal of Mining and Mineral Engineering*, vol. 3, no. 3, pp. 194–219, 2011.

[31] P. A. Lane and D. V. Griffiths, "Assessment of stability of slopes under drawdown conditions," *Journal of Geotechnical and Geoenvironmental Engineering*, vol. 126, no. 5, pp. 443–450, 2000.

[32] M. Neves, V. Cavaleiro, and A. Pinto, "Slope stability assessment and evaluation of remedial measures using limit equilibrium and finite element approaches," *Procedia Engineering*, vol. 143, pp. 717–725, 2016.

[33] G. Sun, S. Cheng, W. Jiang, and H. Zheng, "A global procedure for stability analysis of slopes based on the Morgenstern-Price assumption and its applications," *Computers and Geotechnics*, vol. 80, pp. 97–106, 2016.

[34] S. Y. Liu, L. T. Shao, and H. J. Li, "Slope stability analysis using the limit equilibrium method and two finite element methods," *Computers and Geotechnics*, vol. 63, pp. 291–298, 2015.

[35] D. V. Griffiths and P. A. Lane, "Slope stability analysis by finite elements," *Géotechnique*, vol. 49, no. 3, pp. 387–403, 1999.

[36] J. Shiau and M. M. Hassan, "Numerical modelling of three-dimensional sinkhole stability using finite different method," *Innovative Infrastructure Solutions*, vol. 6, no. 4, p. 183, 2021.

[37] M. R. Maleki, M. Mahyar, and K. Meshkabadi, "Design of overall slope angle and analysis of rock slope stability of chadormalu mine using empirical and numerical methods," *Engineering*, vol. 3, no. 9, pp. 965–971, 2011.

[38] A. Kourdey, M. Aiheib, and J. Piguet, *Evaluation of Slope Stability by Numerical Methods*, vol. 1, pp. 705–710, 2001.

[39] K. H. Head, "Manual of soil laboratory testing," *Effective Stress Tests*, p. 2, John Wiley & Sons, Hoboken, 1998.

[40] A. W. Skempton, "The pore-pressure coefficients a and b," *Géotechnique*, vol. 4, no. 4, pp. 143–147, 1954.

[41] J. T. Christian, C. C. Ladd, and G. B. Baecher, "Closure to "reliability applied to slope stability analysis" by john T. Christian, charles C. Ladd, and gregory B. Baecher," *Journal of Geotechnical Engineering*, vol. 122, no. 5, pp. 417-418, 1996.

[42] K. Terzaghi, R. B. Peck, and G. Mesri, *Soil Mechanics in Engineering Practice*, John Wiley & Sons, Hoboken, 1996.

[43] Y.-S. Song, B.-G. Chae, and J. Lee, "A method for evaluating the stability of an unsaturated slope in natural terrain during rainfall," *Engineering Geology*, vol. 210, pp. 84–92, 2016.

[44] D. G. Fredlund and H. Rahardjo, "Soil mechanics for unsaturated soils," *Soil Mech. Unsaturated Soils*, vol. 12, 1993.

[45] D. G. Fredlund and A. Xing, "Equations for the soil-water characteristic curve," *Canadian Geotechnical Journal*, vol. 31, no. 4, pp. 521–532, 1994.